Comparing Electrochemical Pre-treated 3D Printed Native and Mechanically Polished Electrode Surfaces for Analytical Sensing

Ricoveer Singh Shergill[1, 2], Fernando Perez[1, 2], Aya Abdalla[1, 2], and Bhavik Anil Patel[1, 2*]

[1]School of Applied Sciences, [2]Centre for Stress and Age-Related Disease, Brighton, UK, BN2 4GJ.

*Correspondence should be addressed to Bhavik Patel; Email: b.a.patel@brighton.ac.uk; Tel: +44(0)1273 642418

ABSTRACT

3D printing is a useful and novel approach towards the manufacturing of electrochemical sensors, due to the ability to make electrodes in any geometry. Electrodes made using 3D printers and pens are seldom used as printed. Most commonly, the electrode surface is polished prior to use. We explored the performance of electrochemically pretreated native (where the surface structure of the printed part was not altered) or mechanically polished electrode surfaces made using two different 3D printing manufacturing approaches. Using a 3D printer and pen, electrodes were made using carbon black/polylactic acid (CB/PLA) filament. Post printing, electrodes were used either as printed or following mechanical polishing. Native electrodes made using the printer had a greater response to inner and outer sphere redox probes, enhanced sensitivity, and greater recovery from dopamine fouling than polished printer made electrodes. This trend was completely reserved in pen made electrodes where the performance of polished electrodes was far greater than that of native electrodes. Native electrodes made using the printer were comparable to polished electrodes made using the pen. These results highlight the influence of printing manufacturing approach and electrode preparation to achieve enhanced analytical measurement.

Keywords: 3D printing, Desktop 3D printer, 3D-printing pen, additive manufacturing, electrodes, mechanically polished, native

1. INTRODUCTION

3D printing has revolutionized the approach to make electrochemical sensors [1-7]. Compared to other approaches to manufacture electrodes, 3D printing has provided the ability to make electrodes in any geometry. Complete sensing devices can also be fabricated using 3D printing, where conductive sensing parts are printed alongside non-conductive thermoplastic parts in a single step [8-12]. Such benefits have made 3D printed electrodes an excellent tool for studying environmental, forensic, and biomedical applications [13-19]. Two different approaches to making 3D printed electrodes are used. 3D printers provide excellent resolution and control in making varied electrode geometries[20, 21] however 3D printing pens are easy to use and provide a fast alternative approach to make electrodes [22-24].

At present, post printing 3D-printed surfaces require to be activated to provide sufficient electrochemical activity for analytical sensing. Many treatments can have a profound effect on the electrode surface, however electrochemical pre-treatments provide minimal alteration to the native surface (as printed) of the electrode. Many studies mechanically polish the native surface of the 3D printed electrode using alumina suspension or abrasive paper[25-28]. This process is carried out to ensure that the electroactive material is exposed on the electrode surface. This post-printing process is most widely conducted when making electrodes using 3D pens as the surface is assumed to be more irregular and unreproducible when compared to 3D printer made electrodes[22, 24, 29, 30].

However, the reproducibility in the mass production of native electrodes made through varying approaches of 3D printing is not well known.

Our study explored the performance of electrochemical pre-treated native and polished carbon black/polylactic acid (CB/PLA) electrodes printed by both printer and pen to evaluate their electrochemical activity and performance as electrodes for electroanalysis. Such findings will provide clear insights into the impact of electrode preparation for two different approaches of making 3D printed electrodes when conducting sensing applications.

2. EXPERIMENTAL SECTION

2.1 Fabrication of electrodes using 3D printer and 3D printing pen

Cylindrical electrodes were fabricated using a Creality Ender Pro 3, with a 0.4 mm nozzle at 230 ℃ and a bed temperature of 40 ℃. For the print, 2 shells (outer perimeter toolpaths), 0.1 mm layer thickness, 100 % infill density and speed of 3600 mm/s using CB/PLA filaments (marketed as proto-pasta, was purchased from filaprint, UK) were used. To compensate for the filler content of the material, retractions were disabled, and the extrusion multiplier was set to 1.1. The electrode was printed in a vertical orientation. Our previous studies have showcased that these printing parameters yield conductive materials with enhanced electroactive behaviour [31, 32]. The cylinder was 3 mm in height and 10 mm in diameter. This geometry was chosen as this was deemed to be a suitable dimension that could be made into a native electrode using the printing pen.

Using the 3D printing pen (SUNLU 300) with a 0.75 mm nozzle a cylinder of similar dimensions (10 mm diameter by 3 mm height) was fabricated within a mold made from polydimethylsiloxane. Speed of the 3D-printing pen was 3600 mm/s, and the same carbon black/PLA filament was utilized. **Supplementary video 1** provides an example of the process taken to make the CB/PLA cylinder using the 3D printing pen. The side of the electrode which was in contact with the benchtop surface was explored, given that the other side was compressed in the semi-molten state with mechanical pressure using a spatula. The CB/PLA cylinders made using the printer and pen were then made into electrodes. The cylinders were placed inside an acrylic tube, where electrical connection was achieved by attaching a copper wire using conductive silver epoxy (CircuitWorks) and sealed with Araldite.

Half the batch of printer and pen made electrodes were mechanically activated by manually polishing for 30 s with 1200 grit abrasive paper. Following this the surface electrodes were polished in a figure of eight formation using an alumina suspension of 0.30 μm for a duration 3 minutes. Prior to conducting studies, electrochemical pretreatment was performed on both native and mechanically polished surfaces in 0.5 M NaOH by holding the potential at +1.4 V for 200 s and then at -1.0 V for 200 s [26].

2.2 Scanning electron microscopy (SEM)

The native and polished electrodes made using the 3D printer and pen were imaged using a Zeiss SIGMA field emission gun SEM equipped with an Everhart-Thornley detector operating in secondary electron detection mode, using 5 kV accelerating voltage, a 20 μm aperture, and 8.1 mm working distance.

2.3 Electrochemical characterisation of the 3D printed electrodes

Electrochemical studies were carried out using a three-electrode system, which consisted of a Ag|AgCl (3 M KCl) reference electrode, a platinum wire auxiliary electrode, and the 3D-printed CB/PLA electrode as the working electrode. All electrochemical experiments were carried out using a CH 760E potentiostat (CH instruments, Texas).

Firstly, measurements were conducted in an outer sphere redox probe (1 mM $Ru(NH_3)_6^{2+/3+}$ in 1 M KCl) and inner sphere redox probe (5 mM ferricyanide in 1 M KCl solution). The potential window for $Ru(NH_3)_6^{2+/3+}$ was 0.0 V to -0.5 V and +0.6 to -0.2 V for ferricyanide. Cyclic voltammograms were performed with a scan rate of 0.05 V/s. Mass production of printed electrodes was compared using 6 batches of 6 electrodes. For the electrodes made by the pen, six different researchers made a batch of electrodes.

2.4 Determination of electrode capacitance and resistance

Electrochemical Impedance Spectroscopy (EIS) measurements were performed in a mix of 0.5 mM potassium ferricyanide and 0.5 mM potassium ferrocyanide in 1 M KCl at a potential equal to the anodic peak potential. A frequency range of 100 kHz to 0.01 Hz and an amplitude of 5 mV were utilised. Capacitance was measured in 1 M KCl at varying scan rates, from 30 mV/s to 250 mV/s in the potential window of 0 to +1.0 V and calculations were carried out at +0.5 V.

2.5 Electroanalytical measurements of dopamine

To compare the electroanalytical performance of the 3D printed electrodes, studies were conducted using dopamine. Amperometric calibration in 0.1 to 2.0 µM dopamine in 0.1 M PBS were conducted. Measurements were carried out at +0.65 V.

To explore the stability of the electrodes, the change in the response of 5 mM ferricyanide in 1 M KCl solution was observed after the electrode was exposed to 1 mM dopamine for 10 mins. Following these experiments, the ability to regenerate the electrodes post fouling was explored. To regenerate the electrodes, electrochemical pretreatment was performed in 0.5 M NaOH by holding at +1.4 V for 200s followed by holding at -1.0 V for 200s. Finally, another measurement in 5 mM ferricyanide was carried out to explore if the electrode response had recovered relative to the initial response.

2.6 Data analysis

The cyclic voltammetry measurements were analyzed for anodic/cathodic peak potential, the difference between the anodic and cathodic peak potential (ΔE) and current obtained from the voltammograms using CHI 760E software. The current was utilised to calculate the active surface area using the Randles–Ševčík equation. The heterogenous electron transfer kinetics (HET, k^o) were calculated based on the method by Nicholson as follows.[33]

$$k^o = \Psi \sqrt{(\pi * \frac{nF}{RT} * D * \upsilon)}$$

Where Ψ is dimensionless charge transfer parameter as tabulated by Nicholson [33], R is gas constant (J $K^{-1}mol^{-1}$), T is temperature (K), F is Faraday constant, n is a number of electrons transfer, D is diffusion coefficient (cm^2/s), and υ is scan rate (V/s). The diffusion

coefficient used was 9.1 cm^2/s for $Ru(NH_3)_6^{2+/3+}$. The Nyquist plots were fitted to obtain the R_s and R_{ct} values. To measure the capacitance, the mean difference in anodic and cathodic current (Δi) at 0.5 V was divided by two times the scan rate (2V). This was then normalised by the geometric surface area of the electrode which was 0.785 cm^2 [34]. For amperometric measurements, the current response at varying concentrations of dopamine were obtained.

Data was shown as mean ± the standard deviation (SD). Statistical analysis (GraphPad Prism 9.0) was carried out using student t-tests and two-way ANOVA with Sidak *post hoc* tests.

3. RESULTS AND DISCUSSION

3.1 Comparing the electrochemical pre-treated native and polished CB/PLA electrode surfaces printed by 3D printer and pen

The electrochemical pre-treated did not have significant influence on the surface stucture of the native 3D printed electrode and thus was considered a native surface in the context of electrode surface structure within this study. The surface of the native 3D printed electrode made using the printer had defined printed layers; however, it was difficult to observe structured printed layers on the surface of the native electrode made using the 3D printing pen in the light microscopy and SEM images shown in **Figure 1**. The surface of the electrode made using the pen was mostly flat, where large ridges connected the print layers. This is due to the larger print layer thickness achieved on the 3D pen, where the nozzle is roughly double the size of that present on the 3D printer. The surface of the

electrode made using the 3D printer has significantly more ridges due to the precise 0.1 mm print layers [32].

When the electrodes were polished, a smooth surface over the entire electrode was observed on the electrode that was made using the printer, however large ridges in-between smooth regions were still evident on the polished 3D pen made electrode. From the SEM image for the polished pen made electrode, there is also the presence of voids between the layers (**Figure 1**). After 3 minutes of polishing, the ridges that existed between the 0.1 mm printing layers were completely lost on the printer made electrode, but this duration of polishing was not sufficient to generate a totally smooth electrode surface on the pen made electrode.

Supplementary Figure 1 shows the side view of the native printed cylinder made using the printer and pen. The cylinder made using the pen lacks defined uniform layers and has large ridges between the layers. This suggests that there is a greater likelihood of air voids being present within the cylinder made using the pen and potentially may lead to the electrode being more resistive.

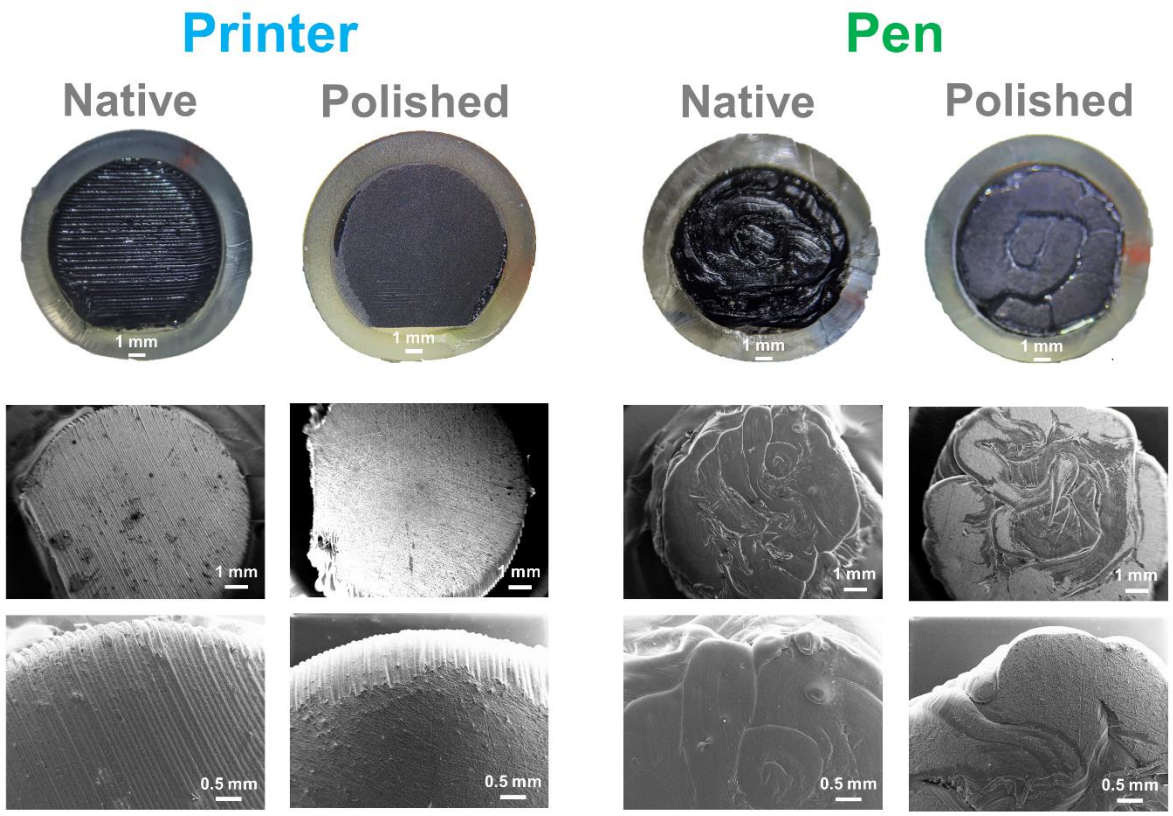

Figure 1. Light microscopy and SEM images of native and polished 3D printed electrodes. Top panel shows light microscopy images, and the next panels show SEM images of the native and polished CB/PLA cylinder made using a 3D printer and pen. The cylinder was placed in an acrylic tube so that only the disc was exposed for electrochemical measurements.

3.2 Electrochemical characterization of native and polished 3D printed electrodes

The 3D printed electrodes were initially electrochemically characterized using two redox couples – outer sphere $Ru(NH_3)_6^{2+/3+}$ and inner sphere ferricyanide. The representative cyclic voltammograms on both electrodes for $Ru(NH_3)_6^{2+/3+}$ is shown in **Figure 2A**. The native electrodes made using the 3D printer exhibited significantly higher cathodic peak currents, lower cathodic peak potential and lower ΔE for $Ru(NH_3)_6^{2+/3+}$ (**Figure 2B-D**,

n=10, p<0.001) when compared to the native pen made electrodes. The polished electrodes made using the printer had significantly lower cathodic peak current and ΔE for $Ru(NH_3)_6^{2+/3+}$ (**Figure 2B&D**, n=10, p<0.001) when compared to the polished pen made electrodes. For the electrodes made using the printer, the native electrodes exhibited a significantly higher cathodic peak current (p<0.001), higher cathodic peak potential (p<0.001) and lower ΔE for $Ru(NH_3)_6^{2+/3+}$ (p<0.01, **Figure 2B-D**, n=10) when compared to the mechanically polished electrodes. For the electrodes made using the 3D pen, the native electrodes exhibited a significantly lower cathodic peak current, higher cathodic peak current and higher ΔE for $Ru(NH_3)_6^{2+/3+}$ (**Figure 2B-D**, n=10, p<0.001) when compared to the mechanically polished electrodes.

The electron transfer rate (k^o), calculated by the Nicholson method, [33, 35, 36] for the native and polished electrodes are shown in **Supplementary Table 1**. When comparing with native electrodes, the k^o was lower on the polished printer made electrodes (p<0.01) but higher on the polished pen made electrodes (p<0.001, n=10). There was a significantly lower k^o for the native pen made electrodes when compared to the native printed electrodes, whilst this trend was reversed in the polished electrodes (P<0.001, n=10).

Using the Randles–Ševčík equation, the active surface of the electrode was calculated and is shown in **Supplementary Table 2**. For the electrodes made using the printer the active native surface area was found to be 0.17 cm^2 (22.4 % of the geometric area), which significantly decreased when the electrodes were mechanically polished (p<0.001, n=10). For the electrodes made using the pen the active surface area was found to be 0.15 cm^2 (19.4 % of the geometric area), however that active surface area

significantly increased following mechanical polishing ($p<0.001$). The active surface is significantly lower than the percentage of CB present within the filament (23 – 30 % by volume) [32] and is suggestive that the reduced active surface area may be due a reduction in the number of conductive pathways in pen and printer made electrodes.

In the native surface, the pen made electrodes has lower electrochemical activity than printer made electrodes, which may be due to poor uniformity of the electrode surface area, reduced surface area and/or higher resistivity due to limited number of conductive pathways. This may be mainly due to the way these electrodes were fabricated given that print layers were perpendicular to the pathway of conductivity, whilst for native 3D printer made electrodes, with a vertical print [31], conductive pathways would be within plane of the print layers. Interestingly, mechanically polishing the electrode reduced the electrochemical activity of the printer made electrodes but improved pen made electrodes. A similar effect was observed in a study using native PLA-graphene electrodes, where a slight decrease in the voltammetric response signal was observed when more than 3 min of polishing was used [28]. The electrochemical activity of the polished pen made electrode is comparable to that of the native printer made electrodes for the measurement of the outer sphere redox probe. This is suggestive that polishing has differential effects on both surfaces, in which polishing printer made electrodes reduced the active surface area of the electrode but increased the availability of the CB in the pen made electrodes.

The representative cyclic voltammograms of both electrodes for ferricyanide is shown in **Figure 2E**. The native electrodes made using the printer exhibited significantly higher anodic peak currents for ferricyanide (**Figure 2F**, $n=10$, $p<0.001$) when compared to the

native pen made electrodes. The polished electrodes which were made using the printer had significantly lower anodic peak currents, higher anodic peak potential and higher ΔE for ferricyanide (**Figure 2F-H**, n=10, $p<0.001$) when compared to the polished pen made electrodes. For the electrodes made using the printer, the native electrode exhibited a significantly lower anodic peak current and potential for ferricyanide ($p<0.01$, **Figure 2F&G**, n=10) when compared to the mechanically polished electrodes. For the electrodes made using the pen, the native electrodes exhibited a significantly lower anodic peak current ($p<0.001$, **Figure 2F**) and higher ΔE for ferricyanide ($p<0.01$, **Figure 2H**, n=10) when compared to the mechanically polished electrodes.

Using the Randles–Ševčík equation, **Supplementary Table 3** shows the active surface of the electrode was calculated based on the measurement of the inner sphere redox probe. The active surface area of the native electrode was significantly increased when mechanically polished on the printer ($p<0.05$, n=10) and pen made electrodes ($p<0.001$, n=10). The active surface area of the native electrodes made by the pen is half that of the electrode made by the printer. The inner sphere probe is more sensitive to the electrode surface and therefore suggests that making electrodes using the printer provides more availability of active sites on the native electrode surface.

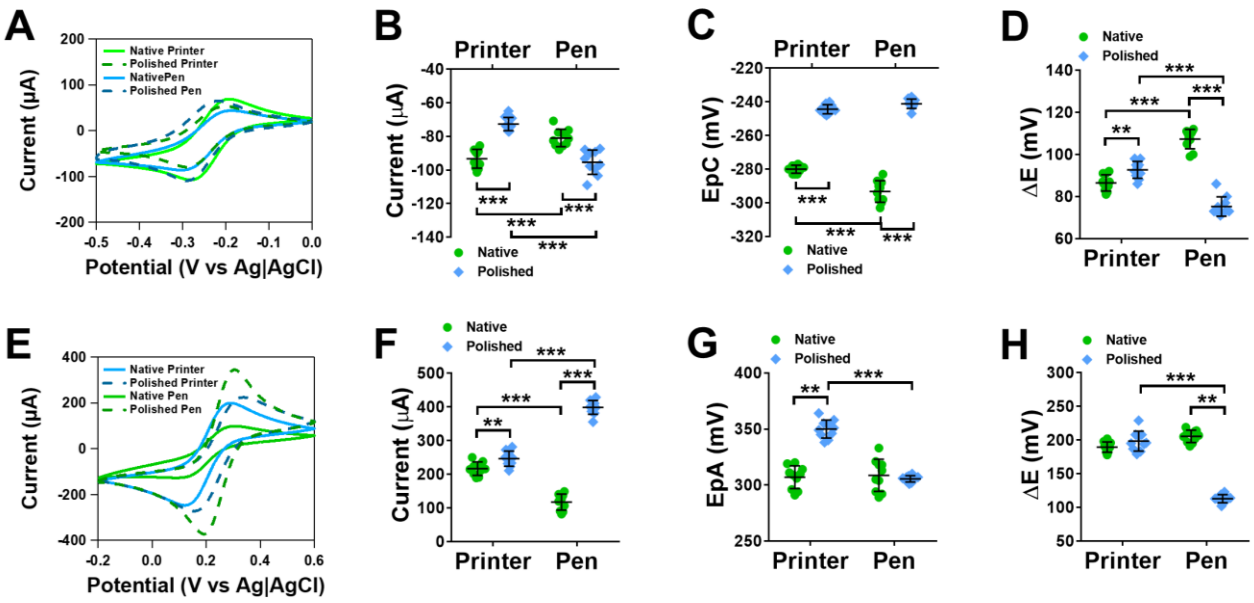

Figure 2. Responses of native and polished 3D printed electrodes on outer and inner sphere redox probes. (A) Representative cyclic voltammograms of 1 mM $Ru(NH_3)_6^{2+/3+}$ in 1 M KCl at 0.05 V s^{-1}, (B) Cathodic current, (C) cathodic peak potential (EpC) and (D) ΔE of $Ru(NH_3)_6^{2+/3+}$. (E) representative cyclic voltammograms of 5 mM ferricyanide in 1 M KCl at 0.05 V s^{-1}, (F) anodic current, (G) anodic peak potential (EpA) and (D) ΔE of ferricyanide. Data shown as mean ± SD, where n = 10, **p<0.01, ***p<0.001.

3.3 Investigating the 3D printed electrode capacitance and resistivity

Since there were significant differences in the voltammetric behaviour between the two electrodes, we subsequently conducted capactiance and impedance measurements to understand the properties of the electrode further.

Electrochemical impedance was utilised to understand the electrode surface and internalized structure of the printed electrodes using a potassium ferric/ferrocyanide mixture.[37-39] From the Nyquist plots for native (**Figure 3A**) and polished (**Figure 3B**)

electrodes printed using the pen and printer, the uncompensated solution resistance (R_s) and interfacial charge-transfer resistance (R_{ct}) was obtained. The R_s significantly increased in the printer made electrodes in both native and polished surfaces when compared pen made electrodes ($p<0.001$, **Figure 3D**, n=6). The R_s significantly increased in polished pen made electrodes when compared to native pen made electrodes ($p<0.05$, n=10). For native electrodes, the R_{ct} was significantly higher in the pen electrodes than the printer made electrodes (**Figure 3E**, n=6, $p<0.001$). In printer made electrodes, the R_{ct} increased in polished electrodes when compared to native electrodes ($p<0.001$, **Figure 3E**, n=6). This trend was reversed in pen made electrodes, where the R_{ct} decreased in polished electrodes when compared to native electrodes ($p<0.001$, **Figure 3E**, n=6).

As capacitance is directly proportional to the electroactive surface area [40], we measured C_{dl} by cyclic voltammetry. Voltammograms obtained at 150 mV/s are shown in **Figure 3C** and mutiple scan rates are shown in **Supplementary Figure 2**. There was a signficant increase in the C_{dl} in the electrode made using the printer when compared to electrodes made using the pen in both the native and polished surface (n=6, $p<0.001$, **Figure 3F**). In the pen made electrodes the C_{dl} significantly increased in the polished electrodes when compared to the native electrodes ($p<0.01$, **Figure 3F**, n=6)

The changes in the R_s would not be expected to change drastically given the measurements were all conducted within the same electrolyte, which may suggest this is possibly an uncompensated resistance related to the volume resistivity of the electrodes. The lower R_{ct} in the native electrodes made by the printer is expected, given this electrode was made in a vertical orientation and we have previously shown that this approach to

manufacturing 3D printer made electrodes removes the effect of air voids between the print layers, which tend to reduce conductivity [32]. However due to the larger print layers in the pen printed electrodes (which is visible in **Figure 1**) and fabrication approach, there is a higher probability that air voids are present, which would reduced the number of conductive pathways present in the electrode. Polishing resulted in a substantial decrease of the R_{ct} and increase in the C_{dl} on pen made electrodes. This suggests the presence of a dielectric film of PLA is more prominent on the surface of native pen made electrodes, which is substantially reduced after polishing. Similar effects have been observed on screen printed Pt electrodes [41].

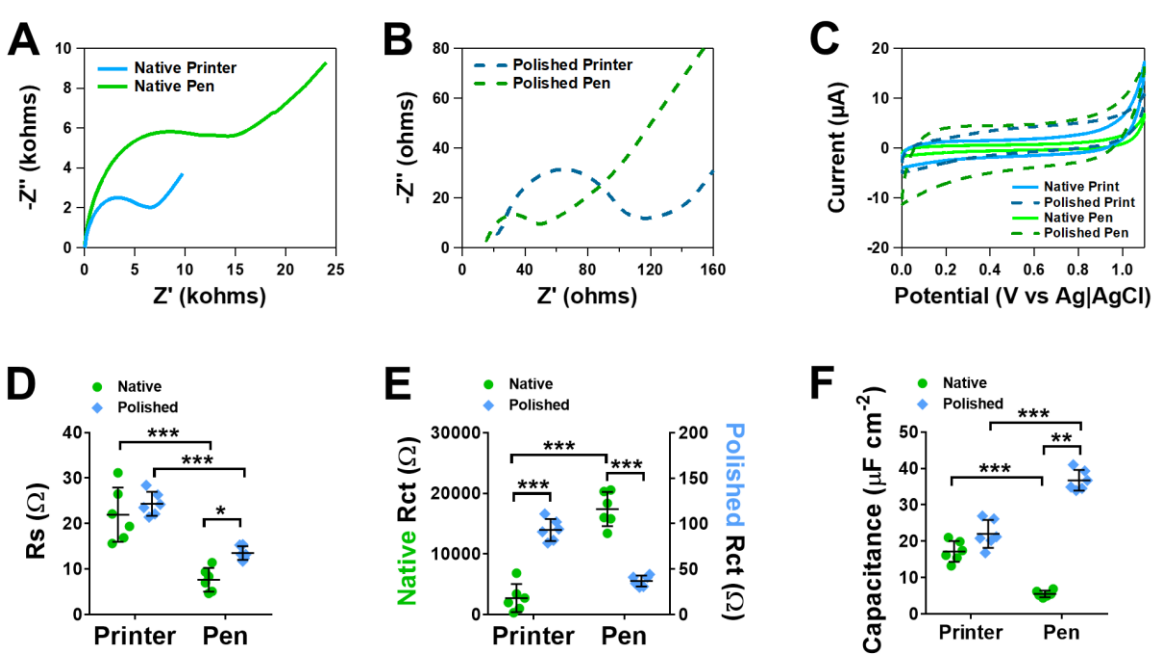

Figure 3. Comparing the resistivity and capacitance of the 3D printed electrodes. Nyquist plots for the native (A) and polished (B) electrodes. Measurements conducted in 0.5 M potassium ferricyanide and 0.5 mM ferrocyanide in 1 M KCl at the mid potential which was 200 mV for native printer and pen, which was 250 mV for polished printer and pen. (C) Cyclic voltammograms in 1

M KCl at 150 mV s^{-1} on a native and polished electrode made using the pen and printer. (D) uncompensated solution resistance (R_s), (E) interfacial charge-transfer resistance (R_{ct}) and (F) capacitance. Data shown as mean ± SD, where n =6, *p<0.05, **p<0.01 and ***p<0.001

3.4 Exploring the mass production of 3D printed electrode made by pen and printer

We evaluated 6 batches (each containing 6 electrodes) in $Ru(NH_3)_6^{2+/3+}$ to explore the mass production capability of the electrodes made using the pen and printer (**Figure 4**). When evaluating the mass production of electrodes made using the printer (**Figure 4A**), there was a significant difference in the cathodic peak current between the bathes (**Figure 4B**, n=6 batches, p<0.001). The % relative standard deviation (RSD) of the cathodic peak current was 3.4 ± 1.1 %. There was no significant difference observed in the cathodic peak potential (**Figure 4C**, % RSD of the cathodic peak potential was 1.1 ± 0.4 %) but there was a significant difference in the ΔE between the batches (**Figure 4D**, n=6 batches, p<0.001). The % RSD of the ΔE was 2.0 ± 0.3 %. To evaluate the mass production of the electrodes made using the pen, each batch was made by a different person (**Figure 4E**). There was a significant difference between the batches when measuring the cathodic peak current of $Ru(NH_3)_6^{2+/3+}$ (**Figure 4F**, n=6 batches, p<0.01). The % RSD of cathodic peak current was 6.0 ± 1.1 %. Similarly, there was a significant difference in the cathodic peak potential (**Figure 4G**, %RSD was 3.1 ± 1.2 %) and ΔE between the batches made using the pen (**Figure 4H**, p<0.01, one-way ANOVA). The % RSD of ΔE was 4.1 ± 0.4 %.

For all the parameters investigated, the %RSD was double for electrode batches made using the pen when compared to the printer. This is expected given the precision of machine manufacturing is far better than human-made manufacturing. However, when comparing these electrodes to other carbon-epoxy composite electrodes which are hand-made by mixing, the precision is significantly improved using the pen and printer [42-47].

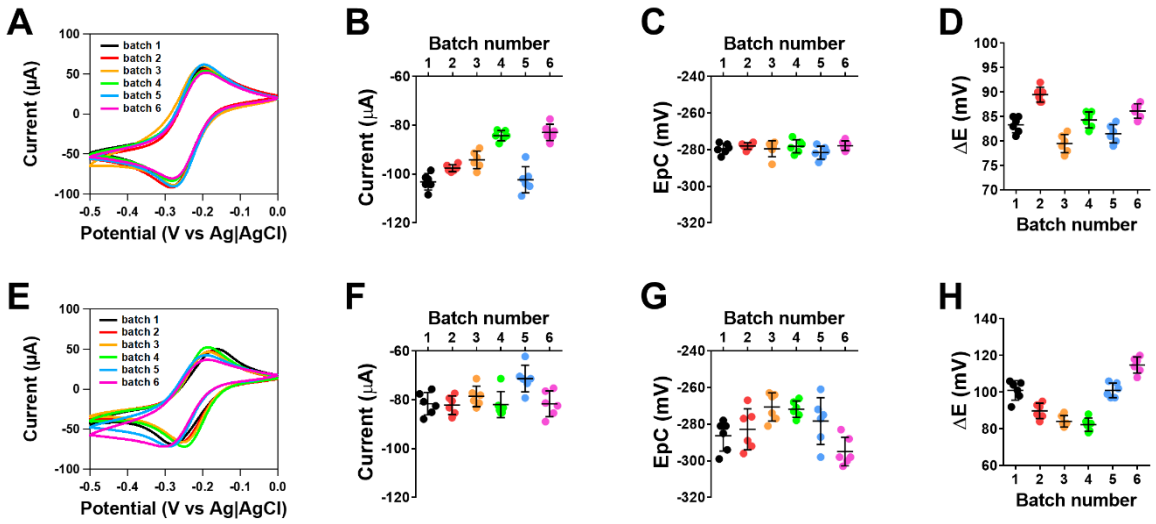

Figure 4. Evaluation of the mass production of the 3D printed electrodes. (A) shows representative cyclic voltammograms of 1mM $Ru(NH_3)_6^{2+/3+}$ in 1 M KCl at 0.1 V s^{-1} from multiple batches made using the printer. (B) shows the cathodic peak current, (C) cathodic peak potential (EpC) and (D) ΔE from the multiple batches made using the printer. (E) shows representative cyclic voltammograms of 1mM $Ru(NH_3)_6^{2+/3+}$ in 1 M KCl at 0.1 V s^{-1} from multiple batches made using the pen. (F) shows the cathodic peak current, (G) cathodic peak potential (EpC) and (H) ΔE from the multiple batches made using the printer. Data shown as mean ± SD, where n = 6 electrodes per batch.

3.5 Performance of 3D printed electrodes for the electroanalytical determination of dopamine

The electroanalytical performance of the electrochemical pre-treated native and polished electrodes which were made using the printer and pen were investigated using the neurotransmitter dopamine.

Figure 5A shows amperometric traces where stable responses were observed over the range of dopamine concentrations explored. The calibration responses for dopamine on the native and polished electrodes made using the printer and pen are shown in **Figure 5B&C**. There was a linear relationship between the current and concentration of dopamine on both native and polished electrodes.

There was a significant increase in the response observed on the native electrodes made by the printer than the pen, whilst this trend was reversed on the polished electrodes ($p<0.001$, two-way ANOVA). The native electrodes made using the printer had the greater response when compared to the polished electrodes. This trend was reversed in the electrodes made using the pen, where the polished electrodes had a significantly greater response ($p<0.001$, two-way ANOVA). The sensitivity on the native electrodes made by the printer was 140 ± 2 nA μM^{-1} whilst the sensitivity was slightly lower at 112 ± 7 nA μM^{-1} (n=6) on the polished electrodes. For the electrodes made using the pen, the sensitivity on the native electrodes was 113 ± 6 nA μM^{-1}, which increased to on the polished electrodes (135 ± 6 nA μM^{-1}, n=6). The responses of the polished printer made electrodes were similar to the native pen made electrodes, whilst the response of the native printer made electrodes was similar to the polished pen made electrodes. The limit of detection (LOD) was defined as 3 times the deviation of the slope from the calibration response.

The LOD for the native electrodes made using the pen was 162 nM, whilst this was slightly lower at 102 nM on the native electrodes made by the printer. An identical pattern was observed for the polished electrodes, where the LOD of the electrode made using the pen was 161 nM and was 109 nM on electrodes made using the printer. These LODs are comparable to other studies conducted with 3D printed electrodes for the determination of dopamine[26, 28] and other neurotransmitters [48].

The analytical performance of the electrode made using the printer in its native surface was comparable to that of the electrode made using the pen when polished, suggestive that 3D printed electrodes require varied preparation to provide sensitive electroanalytical measurements.

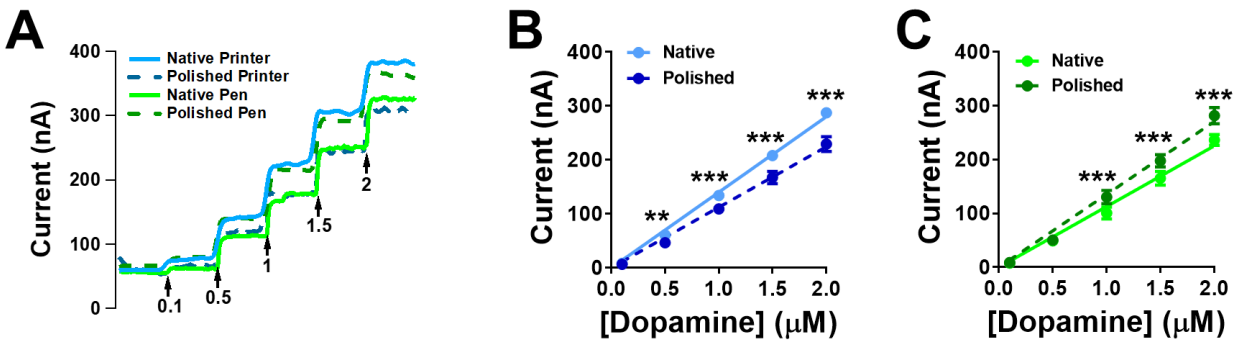

Figure 5. Electroanalytical monitoring of dopamine on printed electrodes. (A) shows representative amperometric traces on native and polished electrodes made using the pen and printer for monitoring of various concentration of dopamine. Values shown in μM. Voltage was held at 0.65 V. Calibration responses on electrodes made using the printer (B) and pen (C). Data shown as mean ± SD, where n =6, **p<0.01 and ***p<0.001.

Stability of electrodes for analytical monitoring is often a major challenge. For the determination of neurotransmitters like dopamine, electrodes are prone to fouling from

oxidative by-products, limiting the lifespan of the electrode[49]. **Figure 6** shows the response of ferricyanide before and after exposure to 1 mM dopamine for 10 minutes. The fouled electrode was then electrochemically treated to determine if it could be regenerated.

For the native and polished electrodes made by the printer and pen representative voltammograms are shown in **Figure 6A-D**. The percentage loss in the anodic peak current of ferricyanide following exposure to 1 mM dopamine for 10 mins was measured is shown in **Figure 6E**. There was no difference in the native printer and pen made electrodes, where approximately ~70 % of the current was lost following fouling from dopamine oxidation. For the electrodes made using the printer, no difference in the degree of fouling between the native and polished electrodes were observed. For the polished pen made electrodes, there was 54 ± 8 % loss in the current response, which was not different to the native pen made electrodes, but significantly lower than the percentage loss on the polished printer made electrodes ($p<0.01$, **Figure 6E**, n=6). Electrochemical pretreatment was used to regenerate the electrode, where significant recovery was observed on all electrodes except that of the polished electrodes made using the printer ($p<0.01$, **Figure 6F**, n=6). When comparing the native electrodes, the electrodes made using the printer had a greater degree of recovery when compared to electrodes made using the pen ($p<0.01$, **Figure 6F**, n=6). However, this trend was reversed on the polished electrodes, where the electrodes made using the pen recovered to a significantly greater extent than that of the printer made electrodes ($p<0.001$, **Figure 6F**, n=6). On electrodes made using the printer, there was a greater recovery observed

on native electrodes than polished electrodes ($p<0.001$, **Figure 6F**, n=6). No difference was observed between the native and polished electrodes made using the pen.

These results indicate that CB/PLA electrodes are prone to fouling, which is expected given the nature of the carbon material and concentration of dopamine used to conduct these measurements. There is a good degree of recovery achieved following electrochemical regeneration on the native electrodes made using the printer and the polished electrodes made using the pen. This recovery may be further improved with multiple or alterative electrochemical activation steps and thus electrodes made using the pen and printer in either the native or polished surface may be fully recoverable.

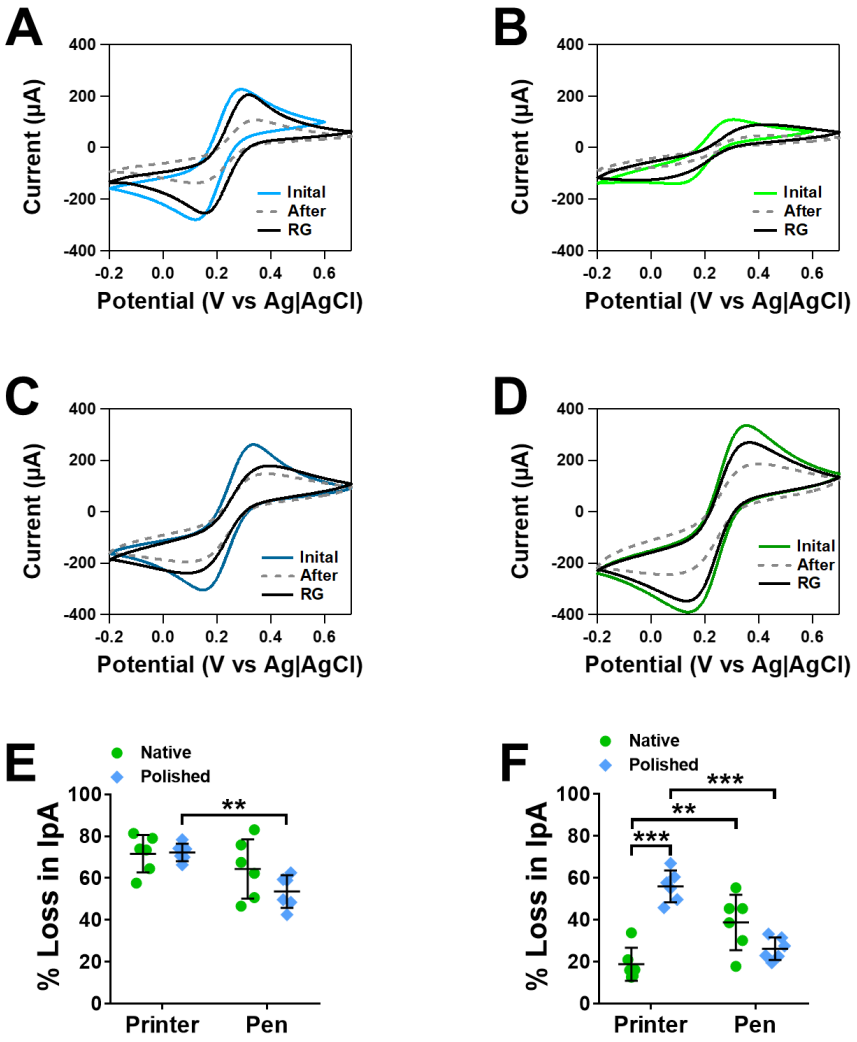

Figure 6. Stability of the printed electrodes when exposed to 1 mM dopamine. Representative voltammograms on the (A) native printer made electrode, (B) native pen made electrode, (C) polished printer made electrode and (D) polished pen made electrode. The stability of the electrode was tracked with redox probe 5mM ferricyanide. (E) percentage loss in the anodic peak current from initial following amperometric measurement at 0.65 V in 1 mM dopamine for 10 mins. Following fouling by dopamine oxidation, electrochemical regeneration (RG) was utilised. (F) percentage loss in the anodic peak current from initial following RG. Data shown as mean ± SD, where n =6, **p<0.01 and ***p<0.001

3.6 Evaluating the strengths and limitations of printed electrodes for analytical measurements

3D printed electrodes can be made using printers and pens and based on the results presented in this study, **Table 1** highlights some of the key differences between these two manufacturing approaches for making electrodes.

Table 1. Comparing the performance parameters of 3D printed electrode made using a printer and pen

Parameter	**Pen**	**Printer**
Printing time	Fast	Medium-Slow
Ability to make into any geometry	Low-Medium	High
Geometry resolution	Low	High
Air pocket density	High	Medium
Inter-operator reproducibility (mass production)	Low	High
Inter-batch reproducibility (mass production)	Low	High

The precision provided by a 3D printer gives greater control in the structural build of the electrode but can be time consuming. These aspects are critical as they can be used to help reduce the air pocket density between the print layers and further enhance the number of conductive pathways present in the final composite printed electrode. Additionally, due to the machine manufacturing, the inter-operator and inter-batch

reproducibility is high. These features naturally help provide enhanced electroanalytical performance for determination of analytes on the native printer made electrodes.

Electrodes using the pen can be made rapidly. However, the ability to generate complex geometries of print is limited to the person-made dexterity in printing but can be improved if using a mold. The inability to make precise structural layers when building the desired geometry will most likely increase the likelihood introducing air pocket voids into the electrode, which in turn reduces the electrochemical activity of the electrode. The inter-operator and inter-batch reproducibility are low, which may not make native pen made electrodes suitable for many analytical applications.

However most surprising in our study was how the performance of the electrochemically pre-treated native electrodes altered when mechanically polished, which is often used to prepare 3D printed electrodes. For the electrode made using the printer, mechanical polishing reduced the sensitivity of the electrode and made the electrode less prone to regeneration following fouling. Similar reductions in performance of printed electrodes when polished have been observed before [28]. This is most likely due to the loss in the surface area from smoothing down the printed layer on the electrode surface. For the electrodes made using the pen, the performance of the sensor significantly improved and matched that of the native printer made electrodes. This is most likely because the dielectric film of PLA present on the native surface is being polished away and thickness of print layers may increase the probability of conductive sites on the electrode surface.

4. CONCLUSIONS

Electrochemical sensors are pivotal analytical tools for chemical measurement. 3D printing has in recent years emerged as an interesting approach to fabricate conductive electrodes of diverse geometries. 3D printers and pens are widely chosen as the main route towards fabrication of electrodes, which can be used as the electrochemical pre-treated native surface or mechanically polished. Our findings highlight that electrochemically pre-treated native electrodes made using a 3D printer have improved precision due to the machine manufacturing when compared to the person-made electrodes using the pen. This in turn improved analytical performance. However, following mechanical polishing, the performance of the 3D pen made electrodes is vastly enhanced and is comparable to the native printer made electrodes. Polishing native printer made electrodes vastly reduce the performance of the electrode. 3D printing manufacturing approach and electrode preparation have significant impact on the electrochemical performance and need to be carefully considered for analytical applications.

Acknowledgements

The authors would like to thank Emma Ward, Nadia Velichkova, Charis Nathan for assisting in making electrodes for batch comparison studies.

Conflict of interest

The authors declare no conflict of interest.

References

[1] A. Ambrosi, M. Pumera, 3D-printing technologies for electrochemical applications, Chem. Soc. Rev., 45 (2016) 2740.

[2] H.H. Hamzah, S.A. Shafiee, A. Abdalla, B.A. Patel, 3D printable conductive materials for the fabrication of electrochemical sensors: A mini review, Electrochemistry Communications, 96 (2018) 27-31.

[3] C.L. Manzanares Palenzuela, M. Pumera, (Bio)Analytical chemistry enabled by 3D printing: Sensors and biosensors, TrAC Trends in Analytical Chemistry, 103 (2018) 110-118.

[4] R.M. Cardoso, D.M.H. Mendonça, W.P. Silva, M.N.T. Silva, E. Nossol, R.A.B. da Silva, E.M. Richter, R.A.A. Muñoz, 3D printing for electroanalysis: From multiuse electrochemical cells to sensors, Analytica Chimica Acta, 1033 (2018) 49-57.

[5] M.R. Khosravani, T. Reinicke, 3D-printed sensors: Current progress and future challenges, Sensors and Actuators A: Physical, 305 (2020) 111916.

[6] R.M. Cardoso, C. Kalinke, R.G. Rocha, P.L. dos Santos, D.P. Rocha, P.R. Oliveira, B.C. Janegitz, J.A. Bonacin, E.M. Richter, R.A.A. Munoz, Additive-manufactured (3D-printed) electrochemical sensors: A critical review, Analytica Chimica Acta, 1118 (2020) 73-91.

[7] M.H. Omar, K.A. Razak, M.N. Ab Wahab, H.H. Hamzah, Recent progress of conductive 3D-printed electrodes based upon polymers/carbon nanomaterials using a fused deposition modelling (FDM) method as emerging electrochemical sensing devices, RSC Advances, 11 (2021) 16557-16571.

[8] V. Katseli, N. Thomaidis, A. Economou, C. Kokkinos, Miniature 3D-printed integrated electrochemical cell for trace voltammetric Hg(II) determination, Sensors and Actuators B: Chemical, 308 (2020) 127715.

[9] V. Katseli, A. Economou, C. Kokkinos, A novel all-3D-printed cell-on-a-chip device as a useful electroanalytical tool: Application to the simultaneous voltammetric determination of caffeine and paracetamol, Talanta, 208 (2020) 120388.

[10] G.D. O'Neil, Toward single-step production of functional electrochemical devices using 3D printing: Progress, challenges, and opportunities, Current Opinion in Electrochemistry, 20 (2020) 60-65.

[11] V. Katseli, A. Economou, C. Kokkinos, Single-step fabrication of an integrated 3D-printed device for electrochemical sensing applications, Electrochemistry Communications, 103 (2019) 100-103.

[12] G.D. O'Neil, S. Ahmed, K. Halloran, J.N. Janusz, A. Rodríguez, I.M. Terrero Rodríguez, Single-step fabrication of electrochemical flow cells utilizing multi-material 3D printing, Electrochemistry Communications, 99 (2019) 56-60.

[13] S.W. Kwok, K.H.H. Goh, Z.D. Tan, S.T.M. Tan, W.W. Tjiu, J.Y. Soh, Z.J.G. Ng, Y.Z. Chan, H.K. Hui, K.E.J. Goh, Electrically conductive filament for 3D-printed circuits and sensors, Applied Materials Today, 9 (2017) 167-175.

[14] M. Pumera, Three-dimensionally printed electrochemical systems for biomedical analytical applications, Current Opinion in Electrochemistry, 14 (2019) 133-137.

[15] A.F. João, A.L. Squissato, E.M. Richter, R.A.A. Muñoz, Additive-manufactured sensors for biofuel analysis: copper determination in bioethanol using a 3D-printed carbon black/polylactic electrode, Analytical and Bioanalytical Chemistry, 412 (2020) 2755-2762.

[16] A. Abdalla, B.A. Patel, 3D-printed electrochemical sensors: A new horizon for measurement of biomolecules, Current Opinion in Electrochemistry, 20 (2020) 78-81.

[17] J. Muñoz, M. Pumera, Accounts in 3D-Printed Electrochemical Sensors: Towards Monitoring of Environmental Pollutants, ChemElectroChem, 7 (2020) 3404-3413.

[18] J.G. Walters, S. Ahmed, I.M. Terrero Rodríguez, G.D. O'Neil, Trace Analysis of Heavy Metals (Cd, Pb, Hg) Using Native and Modified 3D Printed Graphene/Poly(Lactic Acid) Composite Electrodes, Electroanalysis, 32 (2020) 859-866.

[19] S.V.F. Castro, A.P. Lima, R.G. Rocha, R.M. Cardoso, R.H.O. Montes, M.H.P. Santana, E.M. Richter, R.A.A. Munoz, Simultaneous determination of lead and antimony in gunshot residue using a 3D-printed platform working as sampler and sensor, Analytica Chimica Acta, 1130 (2020) 126-136.

[20] J.J. Tully, G.N. Meloni, A Scientist’s Guide to Buying a 3D Printer: How to Choose the Right Printer for Your Laboratory, Analytical Chemistry, 92 (2020) 14853-14860.

[21] A. Abdalla, B.A. Patel, 3D Printed Electrochemical Sensors, Annual Review of Analytical Chemistry, (2021).

[22] F.M. de Oliveira, E.I. de Melo, R.A.B. da Silva, 3D Pen: A low-cost and portable tool for manufacture of 3D-printed sensors, Sensors and Actuators B: Chemical, 321 (2020) 128528.

[23] A.F. João, S.V. Castro, R.M. Cardoso, R.R. Gamela, D.P. Rocha, E.M. Richter, R.A. Muñoz, 3D printing pen using conductive filaments to fabricate affordable electrochemical sensors for trace metal monitoring, Journal of Electroanalytical Chemistry, 876 (2020) 114701.

[24] P.A. Ferreira, F.M. de Oliveira, E.I. de Melo, A.E. de Carvalho, B.G. Lucca, V.S. Ferreira, R.A.B. da Silva, Multi sensor compatible 3D-printed electrochemical cell for voltammetric drug screening, Analytica Chimica Acta, 1169 (2021) 338568.

[25] R.M. Cardoso, P.R.L. Silva, A.P. Lima, D.P. Rocha, T.C. Oliveira, T.M. do Prado, E.L. Fava, O. Fatibello-Filho, E.M. Richter, R.A.A. Muñoz, 3D-Printed graphene/polylactic acid electrode for bioanalysis: Biosensing of glucose and simultaneous determination of uric acid and nitrite in biological fluids, Sensors and Actuators B: Chemical, 307 (2020) 127621.

[26] E.M. Richter, D.P. Rocha, R.M. Cardoso, E.M. Keefe, C.W. Foster, R.A.A. Munoz, C.E. Banks, Complete Additively Manufactured (3D-Printed) Electrochemical Sensing Platform, Analytical Chemistry, 91 (2019) 12844-12851.

[27] R.M. Cardoso, S.V.F. Castro, M.N.T. Silva, A.P. Lima, M.H.P. Santana, E. Nossol, R.A.B. Silva, E.M. Richter, T.R.L.C. Paixão, R.A.A. Muñoz, 3D-printed flexible device combining sampling and detection of explosives, Sensors and Actuators B: Chemical, 292 (2019) 308-313.

[28] C. Kalinke, N.V. Neumsteir, G.d.O. Aparecido, T.V.d.B. Ferraz, P.L. dos Santos, B.C. Janegitz, J.A. Bonacin, Comparison of activation processes for 3D printed PLA-graphene electrodes: electrochemical properties and application for sensing of dopamine, Analyst, 145 (2020) 1207-1218.

[29] R.M. Cardoso, S.V.F. Castro, J.S. Stefano, R.A.A. Muñoz, Drawing Electrochemical Sensors Using a 3D Printing Pen, Journal of the Brazilian Chemical Society, 31 (2020) 1764-1770.

[30] R.M. Cardoso, D.P. Rocha, R.G. Rocha, J.S. Stefano, R.A.B. Silva, E.M. Richter, R.A.A. Muñoz, 3D-printing pen versus desktop 3D-printers: Fabrication of carbon black/polylactic acid electrodes for single-drop detection of 2,4,6-trinitrotoluene, Analytica Chimica Acta, 1132 (2020) 10-19.

[31] H.H.B. Hamzah, O. Keattch, D. Covill, B.A. Patel, The effects of printing orientation on the electrochemical behaviour of 3D printed acrylonitrile butadiene styrene (ABS)/carbon black electrodes, Scientific Reports, 8 (2018) 9135.

[32] A. Abdalla, H.H. Hamzah, O. Keattch, D. Covill, B.A. Patel, Augmentation of conductive pathways in carbon black/PLA 3D-printed electrodes achieved through varying printing parameters, Electrochimica Acta, 354 (2020) 136618.

[33] R.S. Nicholson, Theory and Application of Cyclic Voltammetry for Measurement of Electrode Reaction Kinetics, Analytical Chemistry, 37 (1965) 1351-1355.

[34] K.J. Klunder, Z. Nilsson, J.B. Sambur, C.S. Henry, Patternable Solvent-Processed Thermoplastic Graphite Electrodes, Journal of the American Chemical Society, 139 (2017) 12623-12631.

[35] R.S. Nicholson, I. Shain, Theory of Stationary Electrode Polarography. Single Scan and Cyclic Methods Applied to Reversible, Irreversible, and Kinetic Systems, Analytical Chemistry, 36 (1964) 706-723.

[36] E.P. Randviir, A cross examination of electron transfer rate constants for carbon screen-printed electrodes using Electrochemical Impedance Spectroscopy and cyclic voltammetry, Electrochimica Acta, 286 (2018) 179-186.

[37] E.P. Randviir, C.E. Banks, Electrochemical impedance spectroscopy: an overview of bioanalytical applications, Analytical Methods, 5 (2013) 1098-1115.

[38] S. Vogt, Q. Su, C. Gutiérrez-Sánchez, G. Nöll, Critical View on Electrochemical Impedance Spectroscopy Using the Ferri/Ferrocyanide Redox Couple at Gold Electrodes, Analytical Chemistry, 88 (2016) 4383-4390.

[39] S.D. Keighley, P. Estrela, P. Li, P. Migliorato, Optimization of label-free DNA detection with electrochemical impedance spectroscopy using PNA probes, Biosensors and Bioelectronics, 24 (2008) 906-911.

[40] M. Areir, Y. Xu, R. Zhang, D. Harrison, J. Fyson, E. Pei, A study of 3D printed active carbon electrode for the manufacture of electric double-layer capacitors, Journal of Manufacturing Processes, 25 (2017) 351-356.

[41] J. Lee, D.W.M. Arrigan, D.S. Silvester, Mechanical polishing as an improved surface treatment for platinum screen-printed electrodes, Sensing and Bio-Sensing Research, 9 (2016) 38-44.

[42] A. Fagan-Murphy, S. Kataria, B.A. Patel, Electrochemical performance of multi-walled carbon nanotube composite electrodes is enhanced with larger diameters and reduced specific surface area, J Solid State Electrochem, (2016) 1-8.

[43] A. Fagan-Murphy, B.A. Patel, Compressed multiwall carbon nanotube composite electrodes provide enhanced electroanalytical performance for determination of serotonin, Electrochimica Acta, 138 (2014) 392-399.

[44] H. Zhao, D. Oâ€™Hare, Characterisation and Modeling of Conducting Composite Electrodes, The Journal of Physical Chemistry C, 112 (2008) 9351-9357.

[45] D. O'Hare, J.V. Macpherson, A. Willows, On the microelectrode behaviour of graphite-epoxy composite electrodes, Electrochemistry Communications, 4 (2002) 245-250.

[46] S. Ramírez-García, S. Alegret, F. Céspedes, R.J. Forster, Carbon composite electrodes: surface and electrochemical properties, Analyst, 127 (2002) 1512-1519.

[47] D.E. Tallman, S.L. Petersen, Composite electrodes for electroanalysis: Principles and applications, Electroanalysis, 2 (1990) 499-510.

[48] H.H. Hamzah, O. Keattch, M.S. Yeoman, D. Covill, B.A. Patel, Three-Dimensional-Printed Electrochemical Sensor for Simultaneous Dual Monitoring of Serotonin Overflow and Circular Muscle Contraction, Analytical Chemistry, 91 (2019) 12014-12020.

[49] E. Peltola, S. Sainio, K.B. Holt, T. Palomäki, J. Koskinen, T. Laurila, Electrochemical Fouling of Dopamine and Recovery of Carbon Electrodes, Analytical Chemistry, 90 (2018) 1408-1416.